FEBS Letters 354 (1994) 207–212

FEBS 14694

# The three dimensional structure of rat cytokine CINC/Gro in solution by homonuclear 3D NMR

Hiroyuki Hanzawa[a], Hideyuki Haruyama[a,*], Kazuyoshi Watanabe[b], Susumu Tsurufuji[b]

[a]*Analytical and Metabolic Research Laboratories, Sankyo Co. Ltd., 2-58, Hiromachi 1-Chome, Shinagawaku, Tokyo 140, Japan*
[b]*Institute of Cytosignal Research, Inc., 2-58, Hiromachi 1-Chome, Shinagawaku, Tokyo 140, Japan*

Received 15 June 1994; revised version received 31 August 1994

**Abstract** The solution conformation of rat cytokine-induced neutrophil chemoattractant (CINC/Gro), a small protein consisting of 72 amino acid residues with proinflammatory activities, and a member of the interleukin 8 family corresponding to a counterpart of human Gro, was investigated with homonuclear 2D and 3D NMR spectroscopy. At each phase of the structural analysis, the homonuclear 3D NOESY-HOHAHA and HOHAHA-NOESY spectra afforded valuable data, removing ambiguities intractable by conventional 2D NMR techniques. CINC/Gro exists as a dimer in solution and contains a triple stranded anti-parallel β-sheet and C-terminal α-helix in the monomer structure, as observed in human IL-8, but non-trivial differences are also observed.

*Key words:* Homonuclear 3D NMR; IL-8 family; Three dimensional structure

## 1. Introduction

CINC/Gro is a CXC chemokine belonging to the IL-8 family, and produced by rat renal epithelial cells and normal rat kidney epithelioid cell line NRK-52E [1]. The sequence homologies of CINC/Gro to human Gro and IL-8 are 69% and 47%, respectively. Thus, CINC/Gro was concluded to be the rat equivalent of human Gro [2]. Gro and IL-8 exhibit essentially similar chemotactic properties for neutrophils, but intrinsic diversity of their biological activities may be regulated by specific interaction with different cell surface receptors [3,4]. For example, Gro and IL-8 have quite different affinities to the two types of IL-8 receptors known as type 1 and type 2, which have 74% sequence identity [5]. IL-8 binds to both of the receptors with identical high affinity, while the affinity of Gro to the type 1 receptor is significantly reduced [5].

As for the three dimensional structures of the proteins belonging to the IL-8 family, PF-4 by X-ray crystallography [6] and human IL-8 by both NMR [7,8] and X-ray crystallography [9] are available. These structural studies reveal that PF-4 and IL-8 have similar polypeptide folds and exist as tetramer and dimer, respectively. Recently, the secondary structure of human MGSA/Gro was reported [10]. Knowledge of the three-dimensional structure of CINC/Gro and structural comparisons with the other members are expected to offer basic information in understanding the highly-specific recognition of chemokines by corresponding cell surface receptors in the IL-8 family.

In this study, homonuclear 3D NOESY-HOHAHA and 3D HOHAHA-NOESY spectra have been applied to the structural analysis of chemically synthesized CINC/Gro. At the sequential assignments phase, identification of the secondary structural elements and assignments of the long-range NOEs, 3D homonuclear technique played a decisive role in overcoming the ambiguities due to signal overlapping.

## 2. Materials and methods

CINC/Gro was synthesized chemically in the liquid phase at the Peptide Institute Inc. (Osaka, Japan). Lyophilized samples were dissolved in 90% $H_2O$/10% $D_2O$ or $D_2O$ to give concentrations of 5 mM with 200 mM NaCl at pH 5.3 for NMR measurements.

All 2D and 3D spectra, except when otherwise stated, were recorded at 313K on a JEOL GSX500 spectrometer operating at 500 MHz in the phase-sensitive mode, using the methods of States [11]. The solvent resonance was suppressed by selective irradiation with DANTE pulse during the relaxation delay.

2D Homonuclear Hartman–Hahn spectra were recorded at 303K and 313K with 45 and 60 ms MLEV-17 mixing scheme [12]. The MLEV-17 cycle was preceded and followed by 0.5 ms trim pulse. NOESY spectra [13] were recorded at 303K and 313K with mixing times of 70 and 150 ms.

3D NOESY-HOHAHA and HOHAHA-NOESY spectra were recorded in the phase-sensitive mode as reported in the literature [14,15], except making use of the methods of States in both F1 and F2 dimensions. The mixing time of NOE was 150 ms and that of HOHAHA was 45 ms. The experimental data consisted of 256 × 256 × 1,024 data points and were zero- filled to 512 × 512 × 1,024 points. A total of 8 scans were collected for each increment with repetitive delays of 1 s. The each 3D experiment took 8 days.

All data processing was carried out using NMR2 or NMRZ software on a DEC station 5000/200 computer. The shifted sine bell function was applied to all dimensions. Suppression of undesirable t2 ridges arising from the solvent resonance was achieved by linear baseline correction of the F2 cross section prior to Fourier transformation in t1.

For application of the J doubling technique [16], HOHAHA and NOESY spectra were recorded with data points of 4K.

The three-dimensional structures of CINC/Gro were calculated from the NMR constraints using the programs DIANA [17] and XPLOR [18]. Firstly, monomer structures were calculated from random conformations by DIANA, and then dimer structures were constructed from roughly-folded monomer structures by coordinate duplication, rotation and translation with the knowledge of intersubunit NOEs. In these structures, violations of intersubunit NOEs are about 10–15 Å and no steric hindrance between subunits exists. By using these sets as the initial structures, dynamical simulated annealing calculations were performed [18].

*Corresponding author. Fax: (81) (3) 5436 8567.

*Abbreviations:* DANTE, delays alternating with nutation for tailored excitation; DQF-COSY, double quantum filtered correlated spectroscopy; FID, free induction decay; HOHAHA, homonuclear Hartman–Hahn spectroscopy; MLEV, Malcom Levitt; NMR, nuclear magnetic resonance; NOESY, nuclear Overhauser enhancement spectroscopy.


*SSDI* 0014-5793(94)01081-1

## 3. Results

About 80% of the sequential assignments were achieved using the procedure established by Wüthrich and co-workers [19,20]. The remainder of the sequential assignments were hampered or ambiguous owing to degeneracy of backbone protons. As for $Arg^{8}$ and $Cys^{9}$, where NH signals were degenerated, the sequential connectivities were confirmed by spectra recorded at 303K. However, degenerate chemical shifts of α protons were slightly affected by changing temperature, and hindered continuation of the sequential assignments. This type of difficulty can be overcome using 3D NOESY-HOHAHA spectra. An example is given in Fig. 1a. Since the αH protons of $Glu^{39}$ and $Val^{40}$ have identical chemical shifts, the cross peak for the intraresidue NOE between NH ($Val^{40}$ and aH ($Val^{40}$) coincided with that of the sequential NOE between NH ($Val^{40}$) and αH of ($Glu^{39}$).

These peaks could be resolved on the F2F3 plane, which intersects the F1 axis at F1 = 9.34 ppm, NH($Val^{40}$). Here, the intraresidue NOE of $Val^{40}$ gave cross peak **a** on the back transfer line, because the magnetization of NH($Val^{40}$) was transferred according to the pathway NH($Val^{40}$) $\xrightarrow{NOE}$ αH($Val^{40}$) $\xrightarrow{J}$ NH($Val^{40}$), while the sequential NOE gave cross peak **b** as a consequence of the magnetization transfer following pathway NH($Val^{40}$) $\xrightarrow{NOE}$ αH($Glu^{39}$) $\xrightarrow{J}$ NH($Glu^{39}$). From this NOE, sequential connectivity between $Glu^{39}$ and $Val^{40}$ was unambiguously established.

The sequential NOEs which could be assigned by the 3D technique are as follows: $Gln^{13}$–$Thr^{14}$, $Thr^{14}$–$Val^{15}$, $His^{34}$–$Cys^{35}$, $Glu^{39}$–$Val^{40}$, $Asp^{53}$–$Pro^{54}$ and $Ala^{56}$–$Pro^{57}$. A summary of sequential connectivities is given in Fig. 2 and the chemical shifts are reported in Table 1.

Fig. 2 also contains information on $J_{HN\alpha}$ coupling constants. A broad line width of CINC/Gro hampered accurate measurements of $J_{HN\alpha}$ from DQF-COSY spectra (most of the coupling constants directly measured from DQF-COSY spectra were more than 10 Hz even in the residues involved in the C-terminal α-helix part). Thus, the J doubling method proposed by Freeman et al. was employed.

On the basis of the characteristic short and medium range NOE patterns, secondary structural elements given in Fig. 2 were identified.

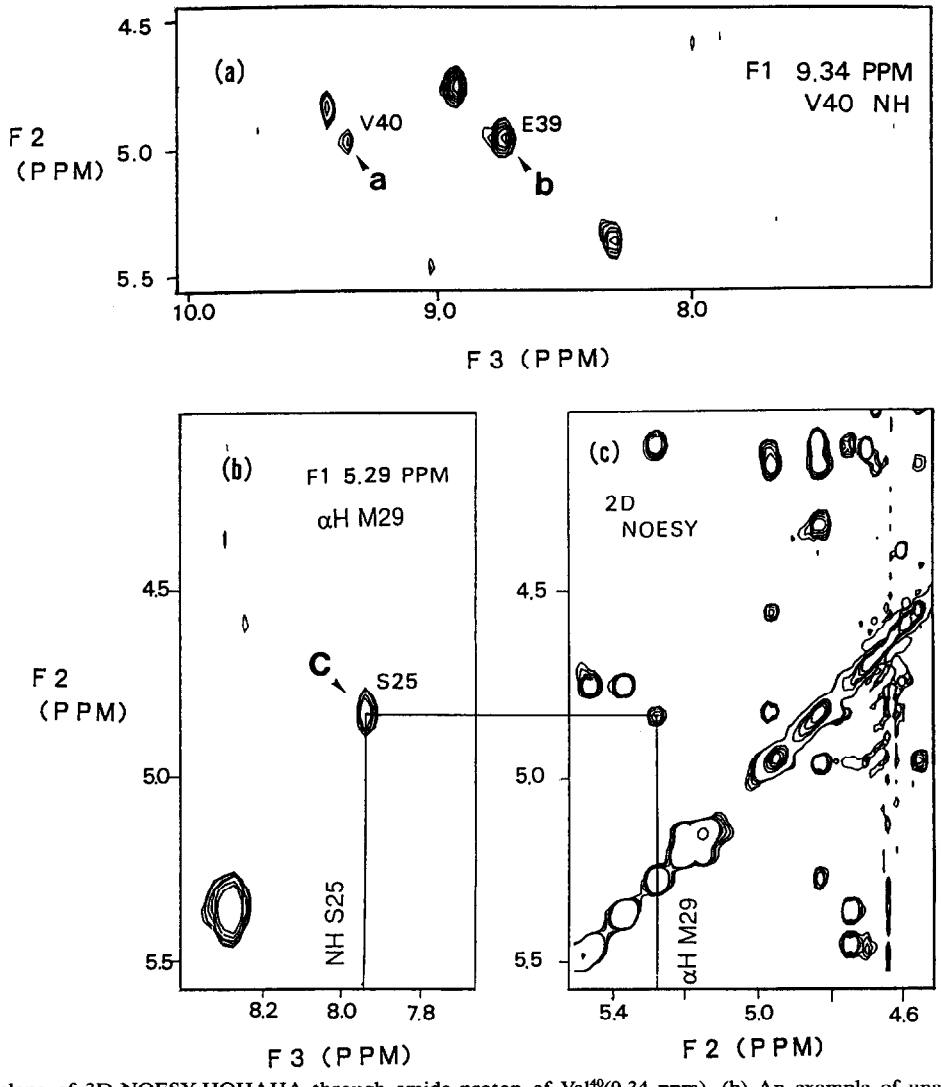


Fig. 1. (a) F2F3 plane of 3D-NOESY-HOHAHA through amide proton of $Val^{40}$(9.34 ppm). (b) An example of unambiguous assignment of intersubunit NOE between αH(S25) and αH(M29). F2F3 plane of 3D NOESY-HOHAHA through F1 = 5.29 ppm (left) and the related region of 2D NOESY spectrum (right) of CINC/Gro are shown.

Table 1
Proton resonance assignment of CINC/Gro at 40 °C at pH 5.3.

| Residue | NH | C α H | C β H | Others |
|---|---|---|---|---|
| A1 | | 4.43 | 1.58 | |
| P2 | | 4.61 | 1.94 2.36 | γ 2.08 δ 3.66 3.77 |
| v3 | 8.21 | 4.16 | 2.12 | γ 1.01 1.01 |
| A4 | 8.34 | 4.34 | 1.43 | |
| N5 | 8.29 | 4.72 | 2.83 2.83 | δ NH 6.85 7.55 |
| E6 | 8.34 | 4.36 | 1.98 2.10 | γ 2.31 2.31 |
| L7 | 8.16 | 4.34 | 1.66 1.66 | γ 1.53 δ 0.93 0.82 |
| R8 | 8.26 | 4.83 | 1.62 1.83 | γ 2.09 δ 3.22 |
| C9 | 8.23 | 4.69 | 3.92 2.74 | |
| Q10 | 11.15 | 4.27 | 2.13 2.13 | γ 2.45 2.45 ε NH 6.74 7.53 |
| C11 | 9.55 | 4.96 | 3.26 2.86 | |
| L12 | 8.61 | 4.36 | 1.71 1.71 | γ 1.71 δ 0.99 0.91 |
| Q13 | 7.76 | 4.71 | 2.07 2.21 | γ 2.36 2.36 ε NH 6.75 7.73 |
| T14 | 8.34 | 4.72 | 4.11 | γ 1.08 |
| V15 | 8.56 | 4.57 | 2.21 | γ 1.03 0.99 |
| A16 | 8.42 | 4.60 | 1.51 | |
| G17 | 7.93 | 3.96 3.96 | | |
| I18 | 7.40 | 4.27 | 1.77 | γ CH2 1.27 1.13 γ CH3 0.77 δ 0.74 |
| H19 | 8.43 | 4.89 | 3.41 3.21 | δ 7.34 ε 8.35 |
| F20 | | 4.02 | 3.32 3.22 | δ 7.18 ε 7.33 ζ 7.25 |
| K21 | 8.34 | 4.09 | 1.94 1.91 | γ 1.43 1.43 δ 1.70 1.70 ε 3.02 |
| N22 | 7.39 | 4.95 | 2.85 3.26 | δ NH 7.03 7.83 |
| I23 | 7.48 | 3.89 | 1.73 | γ CH2 0.72 0.72 γ CH3 0.72 δ 0.62 |
| Q24 | 9.52 | 4.43 | 1.94 1.74 | γ 2.27 2.27 ε NH 6.85 7.41 |
| S25 | 7.42 | 4.85 | 4.12 3.89 | |
| L26 | 8.90 | 5.17 | 1.61 1.61 | γ 1.45 δ 0.92 0.75 |
| K27 | 9.02 | 5.50 | 1.92 1.78 | γ 1.33 1.33 δ 1.53 ε 2.99 |
| V28 | 9.43 | 4.85 | 2.06 | γ 0.88 0.88 |
| M29 | 9.41 | 5.30 | 2.27 2.27 | γ 2.65 2.65 |
| P30 | | 4.98 | 2.30 2.30 | γ 1.96 1.96 δ 3.66 4.12 |
| P31 | | 4.48 | 2.07 2.07 | γ 1.85 1.85 δ 3.56 4.19 |
| G32 | 8.47 | 4.13 4.44 | | |
| P33 | | 4.23 | 1.48 2.27 | γ 2.05 2.05 δ 3.63 3.78 |
| H34 | 8.45 | 4.89 | 3.33 3.11 | δ 7.28 ε 8.52 |
| C35 | 7.41 | 4.93 | 3.06 3.02 | |
| T36 | 8.39 | 4.42 | 4.63 | γ 1.32 |
| Q37 | 7.55 | 4.86 | 2.03 2.25 | γ 2.37 2.44 |
| T38 | 8.57 | 4.58 | 4.01 | γ 1.16 |
| E39 | 8.72 | 4.97 | 2.13 1.97 | γ 2.57 |
| V40 | 9.35 | 4.99 | 2.28 | γ 0.91 0.84 |
| I41 | 9.23 | 4.77 | 1.73 | γ 1.14 1.51 γ CH3 0.81 δ CH3 0.83 |
| A42 | 9.72 | 5.23 | 0.87 | |
| T43 | 8.92 | 4.82 | 4.13 | γ 1.27 |
| L44 | 9.33 | 5.17 | 2.20 2.20 | γ 1.77 δ 0.81 |
| K45 | 8.37 | 4.03 | 1.88 2.00 | γ 1.42 δ 1.79 ε 2.41 |
| N46 | 7.75 | 4.68 | 3.32 2.87 | δ NH 6.56 7.36 |
| G47 | 8.19 | 3.65 4.33 | | |
| R48 | 7.67 | 4.43 | 1.94 1.94 | γ 1.66 1.66 δ 3.25 |
| E49 | 8.29 | 5.39 | 1.95 1.85 | γ 2.35 2.24 |
| A50 | 9.18 | 4.76 | 1.27 | |
| C51 | 8.94 | 4.48 | 3.96 3.13 | |
| L52 | 8.93 | 4.99 | 1.47 1.47 | γ 1.56 δ 0.80 |
| D53 | 8.65 | 4.84 | 2.98 2.68 | |
| P54 | | | | γ 2.15 2.15 δ 4.18 4.34 |
| E55 | 8.00 | 4.24 | 2.03 2.29 | γ 2.46 |
| A56 | 7.77 | 4.69 | 1.71 | |
| P57 | | 4.50 | 1.85 1.85 | γ 2.15 2.15 δ 4.11 4.19 |
| M58 | 8.61 | 4.30 | 2.15 2.34 | γ 2.72 |
| V59 | 7.37 | 3.57 | 2.52 | γ 1.19 0.87 |
| Q60 | 7.58 | 3.84 | 2.20 2.20 | γ 2.39 2.52 6.70 7.60 |
| K61 | 7.85 | 4.08 | 1.91 1.99 | |
| I62 | 8.03 | 3.75 | 2.13 | γ 2.03 1.24 γ CH3 0.95 δ 0.88 |
| V63 | 8.11 | 3.53 | 2.16 | γ 0.99 0.89 |
| Q64 | 7.94 | 3.99 | 2.19 2.19 | γ 2.41 2.53 6.78 7.35 |
| K65 | 8.05 | 3.98 | 1.78 1.66 | γ 1.40 δ 1.36 1.16 ε 2.59 |
| M66 | 8.19 | 4.26 | 2.37 2.37 | γ 2.57 3.02 ε CH3 1.83 |
| L67 | 7.90 | 4.19 | 1.85 1.85 | γ 1.93 δ 0.89 0.84 |
| K68 | 7.66 | 4.30 | 1.86 1.94 | γ 1.53 1.53 δ 1.69 1.69 ε 3.04 |
| G69 | 7.96 | 4.03 4.57 | | |
| V70 | 7.99 | 4.48 | 2.16 | γ 1.05 1.00 |
| P71 | | 4.49 | 2.31 | γ 2.03 2.09 δ 3.75 3.91 |
| K72 | 7.78 | 4.20 | 1.88 1.88 | γ 1.48 1.48 δ 1.76 1.76 ε 3.06 |

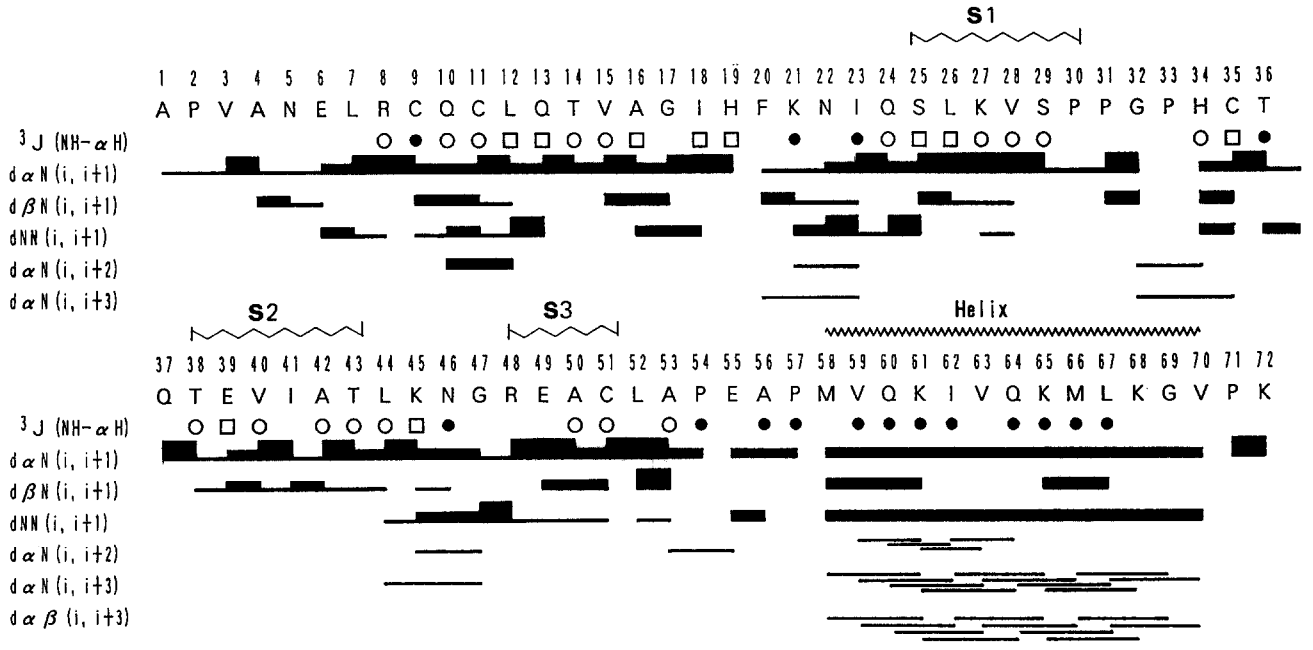


Fig. 2. Amino acid sequence of CINC/Gro and summary of the sequential connectivities used for establishing the sequence-specific $^1$H-NMR assignments. $J_{NH,\alpha}$ coupling constants are classified as follows: J < 6 Hz (●); 6 Hz ≤ J < 8 Hz (□); 8 Hz ≤ J (○).

Fig. 1c exhibits the αH-αH region of a 2D NOESY spectrum recorded in $D_2O$. Based upon the strong αH-αH NOEs appearing in this region, β-strand 1( $Ser^{25}$–$Pro^{30}$), 2 ($Thr^{38}$–$Thr^{43}$), and 3 ($Arg^{48}$–$Cys^{51}$) could be arranged in a triple stranded antiparallel β-sheet.

To identify the β-sheet structures, detection of the array of strong αH-αH NOEs is one of the essential requirements. However, the assignment of a strong NOE observed between αH of $Met^{29}$ and any αH proton at 4.80 ppm was ambiguous in the 2D NOESY spectrum recorded in $D_2O$, because there were three residues with αH protons resonating at 4.80 ppm. Homonuclear 3D NOESY-HOHAHA spectroscopy was useful in differentiating these.

Fig. 1b shows the F2F3 plane of 3D NOESY-HOHAHA which intersects the F1 axis at 5.29 ppm, αH($Met^{29}$). A strong signal was observed at F2 = 4.80 ppm, as a consequence of the magnetization transfer, αH($Met^{29}$) $\xrightarrow{NOE}$ αH(F2 = 4.80 ppm)-$\xrightarrow{J}$ NH(F3 = 7.88 ppm). Since it was $Ser^{25}$ that possessed the NH proton at 7.88 ppm among those residues with αH protons at 4.80 ppm, this NOE could be uniquely assigned to the NOE between αH($Met^{29}$) and αH($Ser^{25}$).

Taking into account the fact that $Ser^{25}$ and $Met^{29}$ are both involved in β strand 1, which forms the antiparallel β-sheet with strand 2, as evidenced by the backbone NOEs, the strong NOE between αH($Met^{29}$) and αH($Ser^{25}$) should be assigned to intersubunit NOE to reconcile with the above mentioned β-sheet structure. Other NOEs such as NH($Leu^{26}$)–NH($Val^{28}$) and NH-($Leu^{26}$)–αH($Met^{29}$) were also interpreted as intersubunit NOEs.

During identification of the β-sheet topology, special care had to be taken to assign the NOEs involving the protons which might be present along the dimer interface, because there was no a priori evidence that CINC/Gro exists as a dimer. Thus it was very important to assign NOEs without depending on the assumed β-sheet arrangement.

The homonuclear 3D technique was also applied to assignments of the long range NOEs. Fig. 3 shows the F1F2 plane of 3D HOHAHA-NOESY spectrum, which intersects the F3 axis at F3 = 7.39 ppm, εH of $Phe^{20}$. The signal **d** on the NOE line shows that NOE was observed between εH of $Phe^{20}$ and one of the protons resonating at 4.25 ppm. Since the set of chemical shifts obtained from the HOHAHA transfer from signal **d** clearly shows that this spin system is $Met^{66}$, **d** could be assigned to a long range NOE between εH($Phe^{20}$) and αH($Met^{66}$). In the same manner, other long range NOEs from εH($Phe^{20}$) to αH,βH($Ile^{62}$) and βH,γH,δH($Lys^{65}$) were easily assigned.

Finally, a set of 613 interproton constraints per monomer and 22 intersubunit NOEs were obtained. The distance constraints consist of 132 intraresidue NOEs and 197 sequential ($|i-j| = 1$), 119 short-range ($1 < |i-j| \leq 5$) and 165 long-range ($5 < |i-j|$) interresidue NOEs. Information on 25 Hydrogen bonds and 40 $\phi$ angle constraints per monomer was used.

The cross peak intensity was quantified based on counting of the evenly-spaced contour levels. Observed NOE data were classified into four distance ranges, 1.8–2.7 Å, 2.5–3.5 Å, 3.0–5.0 Å, and 4.0–6.0 Å, corresponding to strong, medium,weak and very weak.

In the final stage, 500 monomer structures were calculated by DIANA and 50 structures with smallest target function values were accepted. After dimerization and simulated annealing calculations, 20 dimer structures which properly satisfied the constraints, were accepted. In these structures, the distance and torsion angle violations were smaller than 0.3 Å and 10°.

Since only sequential NOEs were observed from $Ala^1$ to $Glu^6$ and $Pro^{71}$ to $Lys^{72}$, these regions are considered to be disordered in solution. From $Leu^7$ to $Val^{70}$ RMSDs about the mean coordinate are 0.94 ± 0.22 Å for backbone atoms and 1.33 ± 0.17 Å for all non-hydrogen atoms.

Fig. 4 shows the stereopair of the best fit superposition of the

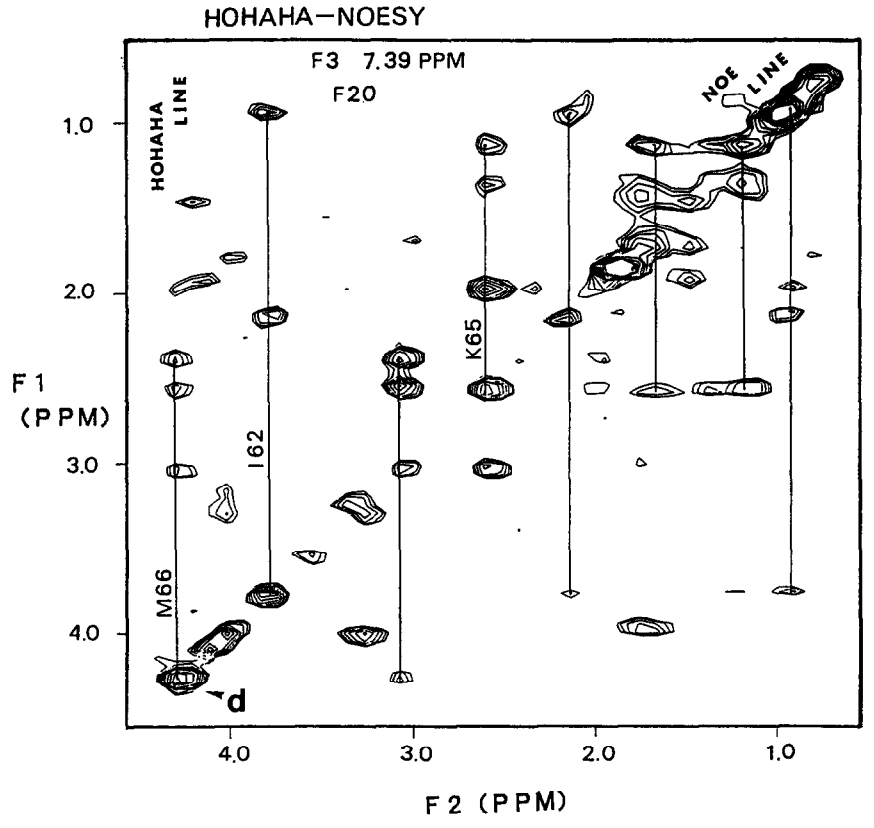


Fig. 3. Application of 3D HOHAHA-NOESY to the assignments of long range NOEs. F2F3 plane of 3D HOHAHA-NOESY through F1 = 7.39 ppm, εH of Phe[20].

backbone atoms for the 20 converged dimer structures. The CINC/Gro monomer consists of a three-stranded antipararell β-sheet and a C-terminal α-helix. In the dimer, the three-stranded β-sheets face each other to form a six-stranded β-sheet.

## 4. Discussion

In the present study, the preliminary three-dimensional structure of CINC/Gro was determined using 2D and homonuclear 3D NMR. 3D homonuclear spectra were found to be especially useful for analyzing overlapping α protons, processing sequential assignments, secondary structure identification and assigning long-range NOEs. In this study, unambiguous NOE assignments independent of the assumed topology were essential to conclude the existence of the dimer structure.

The secondary structural elements of CINC/gro and their relative positions are very similar to those in human IL-8. The arrangement of the dimeric units is identical to those found in human IL-8 and Platelet factor 4 [6,8]. However, differences associated with the secondary structure-breaking properties of Pro residues were detected. The C-terminal α-helix was shortened due to the substitution of two Pro residues at 57 and 71. Furthermore, the Pro residues at 30 and 31 caused the β strands 1 and 2 to shorten, and the loop between them ($Pro^{31}$–$Gln^{37}$) to lengthen, compared with the corresponding structures of human IL-8(31–35).

This long loop region from $Pro^{30}$ to $Thr^{38}$ was not well defined, partly because of the increased flexibility. The existence of the $Pro^{30}$-$Pro^{31}$-X-$Pro^{33}$ sequence resulted in reduced hydrogen bonding with the adjacent chain.

The other long loop region from $Leu^{12}$ to $Ile^{23}$, has many

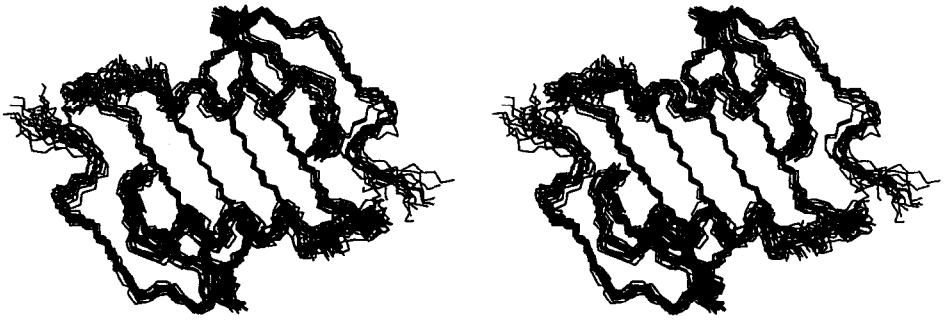

Fig. 4. Stereopair of the superpositions of the 20 converged structures of CINC/Gro. The backbone atoms are shown for the $Leu^{7}$–$Val^{70}$.

hydrophobic contacts with side chains of the α-helix. Side-chain–sidechain NOEs were observed between $Ile^{18}$, $Phe^{20}$ and $Ile^{23}$, and residues of the α-helix. These hydrophobic contacts are thought to play an important role in determining the relative position of the α-helix.

In the CXC-type chemokines, the essential amino acids for neutrophil activation are considered to be the Glu-Leu-Arg sequence in the N-terminal region [21,22]. It is thought that these residues are essential for binding to the receptor on neutrophil. In CINC/Gro, $Glu^6$ has no long-range NOEs and $Leu^7$ has only a few NOEs with C2 of $His^{34}$. Thus, no rigid conformation was determined, as in the case of human IL-8, and the Glu-Leu-Arg region is considered to be flexible like human IL-8.

For a more detailed comparison, with special interest in the effects of reduced hydrogen bonding along the dimer interface and truncated C-terminal α-helix on the dynamical aspects of protein structure, the high-resolution structure of CINC/Gro is needed. To achieve this, we have prepared isotope-labeled CINC/Gro and analysis is in progress.

## References

[1] Watanabe, K., Kinoshita, S. and Nakagawa, H. (1989) Biochem. Biophys. Res. Commun. 161, 1093–1099.
[2] Watanabe, K., Konishi, K., Fujioka, M., Kinoshita, S. and Nakagawa, H. (1989) J. Biol. Chem. 264, 19559–19563.
[3] Horuk, R., Yansura, D.G., Relly, D., Spencer, S., Bourell, J., Henzel, W., Rice, G. and Unemori, E. (1993) J. Biol. Chem. 268, 541–546.
[4] Loetscher, P., Seitz, M., Lewis, I.C., Buggiolin, M. and Moser, B. (1994) FEBS Lett. 341, 187–192.
[5] Cerretti, D.P., Kozlosky, C.J., Vanden, B.T., Nelson, N., Gearing, D.P. and Beckman, P. (1993) Mol. Immunol. 30, 359–367
[6] St. Charles, R., Walz, D.A. and Edwards, B.F.P. (1989) J. Biol. Chem. 264, 2092–2099.
[7] Clore, B.M., Appella, E., Yamada, M., Matsushima, K. and Gronenborn, A.M. (1989) J. Biol. Chem. 264, 18907–18911.
[8] Clore, B.M., Appella, E., Yamada, M., Matsushima, K. and Gronenborn, A.M. (1990) Biochemistry 29, 1689–1696.
[9] Baldwin, E.T., Weber, I.T., St. Charles, R., Xuan, J.C., Appella, E., Yamada, M., Matsushima, K., Edwards, B.F.P., Clore, G.M., Gronenborn, A.M. and Wlodawer, A. (1991) Proc. Natl. Acad. Sci. USA 88, 502–506.
[10] Fairbrother, W.J., Reilly, D., Colby, T. and Horuk, R. (1993) FEBS Lett. 330, 302–306.
[11] States, D.J., Haberkorn, R.A. and Ruben, D.J. (1982) J. Magn. Reson. 48, 286–292.
[12] Bax, A. and Davis, D.G (1985) J. Magn. Reson. 65, 355–360.
[13] Jeener, J., Meier, B.H., Bachmann, P. and Ernst, R.R. (1979) J. Chem. Phys. 71, 4546–4553.
[14] Vuister, G.W., Boelens, R. and Kaptein, R. (1989) J. Magn. Reson. 80, 176–185.
[15] Vuister, G.W., deWaard, P., Boelens, R., Vliegenthart, J.F.G. and Kaptein, R. (1989) J. Am. Chem. Soc. 111, 772–774.
[16] Mcintyre, L. and Freeman, R. (1992) J. Magn. Reson. 96, 413–425.
[17] Guntert, P., Braun, W. and Wüthrich, K (1991) J. Mol. Biol. 217, 517–530.
[18] Nilges, M., Clore, G.M. and Gronenborn, A.M. (1988) FEBS. Lett. 229, 317–324.
[19] Billester, M., Brawn, W. and Wüthrich, K. (1982) J. Mol. Biol. 155, 321–346.
[20] Wagner, G. and Wüthrich, K. (1982) J. Mol. Biol. 155, 347–366.
[21] Clark-Lewis, I., Schumacher, C., Baggiolini, M. and Bernhard, M. (1991) J. Biol. Chem. 226, 23128–23134.
[22] Hebert, C.A., Vitangcol, R.V. and Baker, J.B. (1991) J. Biol. Chem. 266, 18989–18994.